

Image Generation from Contextually Contradictory Prompts

Saar Huberman¹ Or Patashnik¹ Omer Dahary¹ Ron Mokady² Daniel Cohen-Or¹

¹Tel Aviv University ²BRIA AI

<https://tdpc2025.github.io/SAP/>

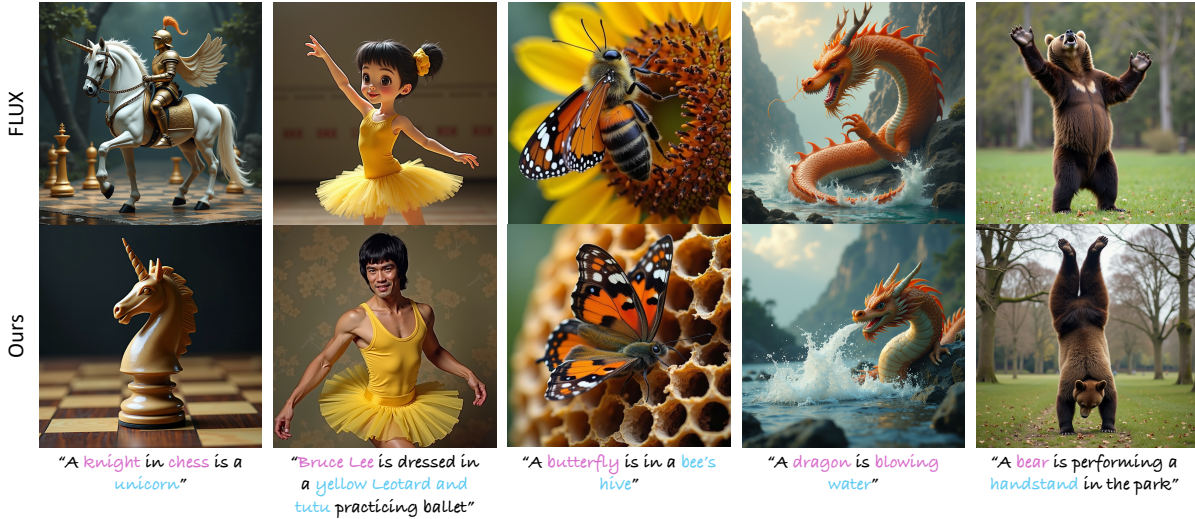


Figure 1. Our method addresses contextual contradictions in text-to-image generation. These contradictions arise when one concept implicitly conflicts with another due to the model’s learned associations. For example, if a concept like “butterfly” is strongly entangled with “flowers”, it may conflict with another concept in the prompt such as “bee’s hive”, leading the model to ignore or distort part of the semantic meaning.

Abstract

Text-to-image diffusion models excel at generating high-quality, diverse images from natural language prompts. However, they often fail to produce semantically accurate results when the prompt contains concept combinations that contradict their learned priors. We define this failure mode as contextual contradiction, where one concept implicitly negates another due to entangled associations learned during training. To address this, we propose a stage-aware prompt decomposition framework that guides the denoising process using a sequence of proxy prompts. Each proxy prompt is constructed to match the semantic content expected to emerge at a specific stage of denoising, while ensuring contextual coherence. To construct these proxy prompts, we leverage a large language model (LLM) to analyze the target prompt, identify contradictions, and generate alternative expressions that preserve the original intent while resolving contextual conflicts. By aligning prompt information with the denoising progression, our method enables fine-grained semantic control and accurate image generation in the presence of contextual contradictions. Experiments across a variety of challenging prompts show substantial improvements in alignment to the textual prompt.

1. Introduction

Text-to-image diffusion models have demonstrated remarkable capabilities in generating high-quality and diverse visual content from natural language prompts [15, 24, 27]. However, achieving precise semantic alignment between the generated image and the conditioning prompt remains an open challenge. This issue becomes particularly pronounced when the target prompt lies outside the model’s training distribution, such as prompts that combine semantically plausible yet statistically uncommon or unconventional concepts. For example, as shown in Figure 1, generating an image from the prompt “A butterfly is in a bee’s hive” often results in a butterfly on a flower. This is due to the model’s prior that entangles butterflies with flowers, which implicitly contradicts the notion of a bee’s hive.

We refer to this phenomenon as *Contextual Contradiction*, a conflict between two concepts that arises not from direct semantic opposition, but from the model’s associations learned during training. More precisely, we say that concept A contextually contradicts concept B if the model’s prior entangles A with concept C , and B contradicts C (see Figure 2). In Figure 1, we illustrate this with a blowing dragon, which stands in contextual contradiction with the water due to its entanglement with fire.

The phenomenon of contextual contradiction in text-to-

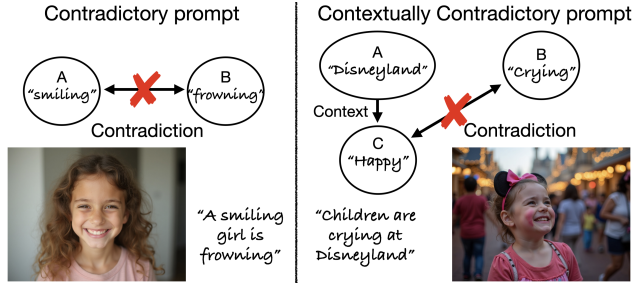


Figure 2. On the left is a direct contradiction, since a girl cannot smile and frown at the same time. On the right is a contextual contradiction: while Disneyland and crying are not directly opposed, the model’s prior associates Disneyland with happiness, which conflicts with crying.

image models relates to the broader issue of spurious correlations in deep learning. Models often exploit shortcuts, relying on correlations in the training data that are statistically strong but semantically misleading [13]. In this paper, we identify a similar bias in generative models: contextual contradictions occur when prompts combine concepts that individually align with the model’s priors but conflict when combined, revealing the model’s reliance on such correlations rather than robust compositional reasoning.

To address this issue, we introduce *Stage-Aware Prompting (SAP)*, which builds on the observation that the denoising process follows a coarse-to-fine progression, during which different semantic attributes (e.g., background, pose, shape, and texture) emerge at distinct stages [4, 9, 23]. Our key idea is to guide the model at each stage of denoising with the information most relevant to the type of content being formed at that point. To achieve this, we decompose the original prompt into a sequence of proxy prompts, each aligned with the attributes expected at a specific stage and designed to avoid contextual contradictions.

Ensuring that proxy prompts preserve the original intent while avoiding contextual contradictions requires a broad understanding of the real world. For example, it involves understanding that a bear is entangled with specific poses, such as walking on all fours or standing upright, which in turn, contradicts the handstand pose. To achieve this, SAP leverages a large language model (LLM) to analyze the target prompt, identify contextual contradictions, and construct suitable proxy prompts.

We demonstrate that, by using in-context examples and prompting the LLM to follow a reasoning process through a brief explanation, it can identify contextually contradictory concepts in a prompt and determine the appropriate stage of denoising at which each attribute should be introduced. It can also suggest alternative, non-conflicting concepts that preserve the intended attributes and use them to construct stage-specific proxy prompts. In doing so, the LLM effectively guides the model toward the intended meaning of the original prompt.

Through extensive experiments, we demonstrate the effectiveness of SAP in generating images from contextually contradictory text prompts. By introducing prompt information at targeted stages, SAP generates precise combinations of semantic attributes while avoiding undesired entanglement. Compared to previous methods, SAP’s stage-dependent prompt decomposition leads to more faithful and semantically aligned generations.

2. Related Work

Learned Spurious Correlations. Machine learning models are known to be sensitive to spurious correlations in their training data [13, 20, 33], leading to performance drops when training-time associations do not hold at test time. Prior work has extensively studied this in discriminative vision tasks, showing, for example, that recognition models tend to rely heavily on background cues [6, 28, 31]. In our work, we show that text-to-image models exhibit similar behavior. When given contextually contradictory prompts – combinations of concepts that conflict with correlations seen during training – diffusion models often fail to generate images that accurately reflect the prompt. We evaluate this behavior using the Whoops! dataset [7], which contains prompts constructed by first describing two co-occurring elements, and then replacing one with a less compatible alternative. This results in scenarios that are unlikely to occur in the real world.

Semantic Alignment in Text-to-Image Synthesis. Text-to-image models often struggle to fully capture the semantic intent of input prompts, particularly when prompts involve complex or internally conflicting concepts. Previous works have analyzed common failure cases and proposed targeted improvements across various stages of the generation pipeline, including enhanced text embedding representations [12, 25, 29], refined attention mechanisms [10], guidance strategies that leverage attention maps for loss heuristics [2, 9, 21, 26] and dynamic guidance scheduling via annealed classifier-free guidance [34]. Despite these advances, existing methods often fail to handle prompts containing contradictory concepts arising from the model’s learned associations. Our work directly addresses this underexplored challenge, focusing on contextually contradictory prompts.

Multi-Prompt Conditioning Techniques. Conditioning diffusion models on multiple prompts has emerged as an effective strategy for improving control and compositionality. One line of work, primarily focused on personalization, introduces distinct learned tokens at different layers of the model and at various denoising timesteps [3, 30]. This design allows each token to capture different attributes of the personalized concept, leading to improved identity preservation. Other approaches vary the prompt across timesteps

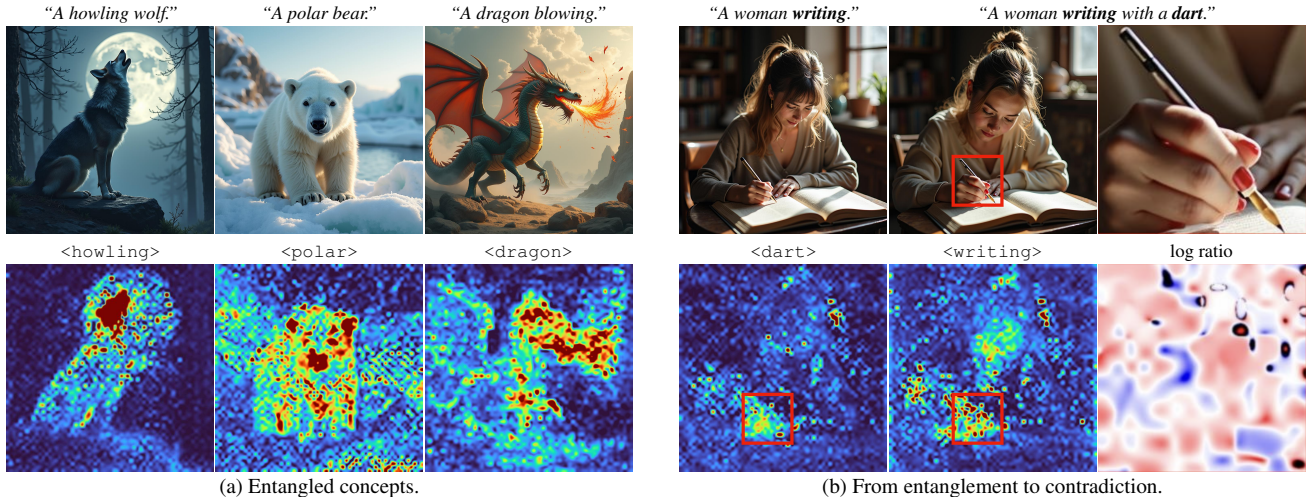


Figure 3. (a) By examining attention maps, we observe that textual tokens embed contextual associations, leading to the generation of concepts not explicitly mentioned in the prompt. For example, the token ‘howling’ encourages the presence of the moon, as indicated by its strong attention connection. (b) In prompts with contextual contradictions, two tokens may overlap in attending to the same region, as seen with ‘dart’ and ‘writing’. The token ‘writing’ dominates this region, as shown in the log-ratio map, where red areas indicate stronger attention to ‘writing’ relative to ‘dart’.

to modulate specific visual properties, such as object shape [18, 23], or alternate between rare and frequent object descriptions to improve attribute binding [22]. Fine-grained spatial control has also been achieved by assigning sub-prompts to separate image regions [32]. Additionally, some methods leverage multiple diffusion models, each conditioned on different prompt attributes, and combine their outputs into a unified prediction [5, 19]. Unlike most prior works, we focus on utilizing multiple prompts to settle internal semantic tension, where concept combinations lead to contextual contradictions.

LLM-Guided Diffusion. LLMs have demonstrated strong capabilities in language understanding. They also capture broad world knowledge through large-scale training on diverse text. Recent approaches have leveraged these capabilities to guide diffusion model generation, often incorporating planning and reasoning to improve semantic alignment [16, 22, 32]. In our work, we employ LLMs with in-context learning to identify contextual contradictions, generate proxy prompts, and determine the corresponding timestep ranges for conditioning, while encouraging reasoning through brief explanatory outputs.

3. From Entangled Concepts to Contextual Contradictions

Diffusion models inherit strong distributional biases from their training data, where objects are frequently tied to specific contexts. For example, prompts like “a duck” almost always result in water backgrounds, and “a polar bear” appears in snow. These reflect *entangled concepts*, learned associations that go beyond the explicit text. While often

helpful, such priors hinder generation when prompts require unusual or contradictory combinations.

To study this effect, we analyze attention maps (Figure 3a), which indicate the spatial regions influenced (attended) by each token. We find that text tokens often attend not only to the image regions directly corresponding to the object but also to contextually linked elements. For example, in “a howling wolf”, the token ‘howling’ influences both the mouth and the moon. Similarly, ‘dragon’ attends to flames even when fire is not mentioned. These patterns reveal that the model encodes distributional correlations beyond literal semantics.

These distributional correlations contribute to the difficulty of generating images with *contextual contradictions*. For example, when generating an image from the prompt “a woman writing with a dart”, the model fails to replace the pen with a dart. The attention maps shed light on this failure: both ‘writing’ and ‘dart’ attend to the same spatial area (the hand/tool), but ‘writing’ dominates (see log-ratio maps in Figure 3b), suppressing the influence of ‘dart’. This reflects a failure mode in which entrenched associations override less familiar ones, preventing proper integration of conflicting concepts.

4. Stage Aware Prompting (SAP)

In this section, we begin by analyzing the coarse-to-fine behavior of the denoising process (Section 4.1). Building on the insights from our analysis, we introduce our training-free framework for resolving contextual contradictions in text-to-image generation. As illustrated in Figure 5, our approach consists of two main components: (i) prompt decomposition (Section 4.2, top part of the figure), and (ii)



Figure 4. *Coarse-to-fine denoising with stage-aware prompting.* We show x_0 predictions at initial, intermediate, and final steps. A is the target prompt, B a suitable proxy, and C an unsuitable proxy. Using A alone locks in night and moon despite “midday”. Using B first and then switching to A preserves a daytime layout and later adapts the identities to wolf and bat. Using C first sets a layout without a flying object, so the final image fails to produce the intended subjects.

stage-aware prompt injection (Section 4.3, bottom part of the figure). In the following, we describe each of these components.

4.1. Coarse-to-Fine Denoising

Diffusion models generate images in a coarse-to-fine manner: early steps determine low-frequency structures, while high-frequency details emerge in later steps [4, 9, 14, 23]. From this behavior, we draw two key observations: (i) *Irreversibility of details.* As denoising progresses, the model sequentially commits to different levels of detail, beginning with layout and overall shape. Once these are formed, they cannot be revised in later stages, even if they conflict with the prompt. (ii) *Flexibility in high-frequency details.* In early stages, high-frequency details are absent and unaffected by the prompt, enabling flexible guidance without influence on fine details.

As shown in Section 3, contextual contradictions stem from concept entanglement in the diffusion prior. Since different concepts emerge at different levels of detail during the coarse-to-fine denoising process, they can be decomposed across the denoising stages. We illustrate this in Figure 4 by examining the model’s x_0 predictions across denoising steps. In the top-left row, the prompt “a howling wolf and a flying bat at midday” shows that early steps already impose entangled nighttime and moon structures, contradicting “midday”. In the bottom-left row, starting with a *proxy prompt* containing “dog” and “bird” (instead of “wolf” and “bat”, respectively) and later switching to the target prompt produces a correct midday scene with the intended objects. The bottom-left row demonstrates both the *irreversibility of coarse details* (the scene remains daytime) and the *flexibility of high-frequency details* (the object identities adapt). The top-right row highlights the importance

of selecting an appropriate proxy prompt. Since rats do not fly, the layout determined in early steps lacks a flying object, resulting in a sitting wolf with bat wings.

These observations motivate a stage-aware prompting strategy that fixes structural decisions early while keeping later attributes flexible. Building on this, we now describe the two main components of our method: prompt decomposition and stage-aware prompt injection.

4.2. Prompt Decomposition

Given a prompt P that contains contextually contradictory concepts, we aim to construct a sequence of proxy prompts $\{p_1, p_2, \dots, p_n\}$ and corresponding timestep intervals $\{I_1, I_2, \dots, I_n\}$ that together reflect the intended semantics of P . Each proxy prompt p_i is designed to (i) preserve the relevant semantics of P for attributes typically formed during its interval I_i , which is crucial due to the *irreversibility of details*, and (ii) avoid contradictions likely to emerge at that stage, leveraging the *flexibility in high-frequency details*. This decomposition conditions the diffusion model on contextually coherent content that evolves in tandem with the coarse-to-fine denoising process.

To generate proxy prompts and their intervals, we use a large language model (LLM) that detects contextual contradictions and proposes suitable substitutes for conflicting concepts. It also infers the appropriate staging of these concepts within the proxy prompts. We implement this using a structured prompt template containing instructional text, in-context examples, and explanations of contextual contradictions. The examples demonstrate both successful decompositions and cases requiring no decomposition, enabling the LLM to generalize. The full instruction prompt is provided in the Appendix.

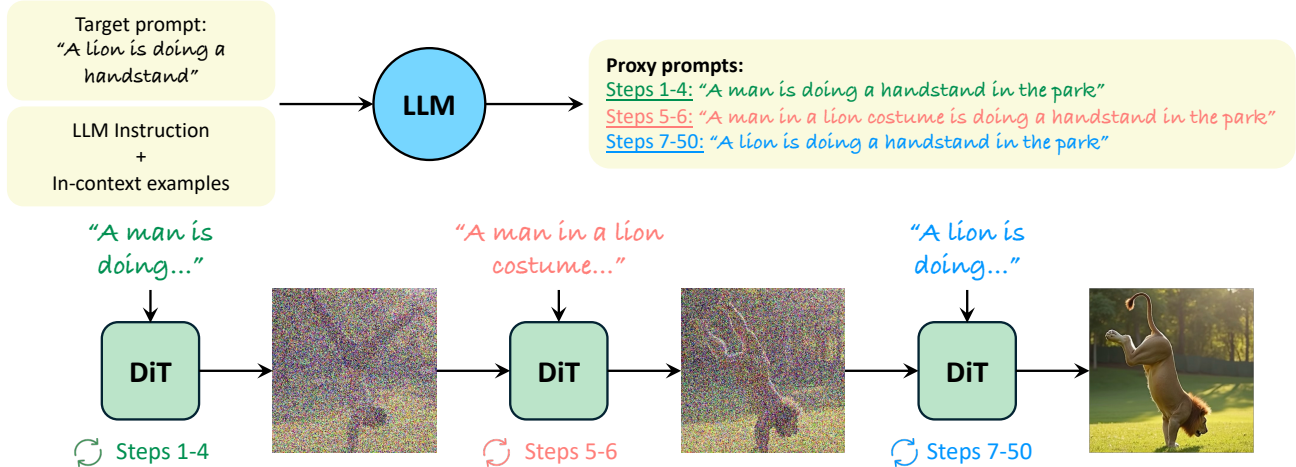


Figure 5. SAP generates images from contextually contradictory prompts using time-dependent proxy prompts. (Top) A large language model (LLM) decomposes the target prompt into a sequence of proxy prompts with corresponding timestep intervals. (Bottom) These proxy prompts are injected into the diffusion process at their designated intervals to guide generation.

In-context Examples. Our in-context examples take a target prompt as input and output proxy prompts with timestep intervals, along with a brief explanation of the contradiction. Requiring the LLM to provide this explanation encourages reasoning about conflicts and ensures coherent substitutions. These examples were created by identifying contextually contradictory prompts that fail under the base model (FLUX) and manually decomposing them into proxy prompts with corresponding intervals. The explanations were auto-generated by an LLM. We include 20 examples that demonstrate diverse strategies for handling contradictions. We next elaborate on one of the most frequent strategies in our method.

Concept Substitution. In this strategy, a conflicting concept is temporarily replaced with a structurally appropriate proxy (Figure 4). A simpler alternative is to omit the conflicting concept, but introducing an object only in later stages without a placeholder can distort its perceived size or cause it to be omitted entirely. In Figure 6, we demonstrate this by comparing decompositions that differ only in when the second interval begins. The first proxy specifies the background, while the second adds the foreground. Introducing the foreground early allows the model to allocate more space, whereas delaying it constrains the layout and produces a smaller object. Substitution resolves these issues and yields stable layouts. In Figure 7, we show the effect of misplacing intervals across denoising stages. Using two proxies with different intervals, where the second is the full prompt, we observe two failure modes: introducing the full prompt too early prevents disentangling contradictions, while introducing it too late alters only fine details. Earlier in Figure 4 we illustrated the importance of careful proxy selection.

4.3. Stage-aware Prompt Injection

Given a sequence of proxy prompts $\{p_1, p_2, \dots, p_n\}$, their corresponding timestep intervals $\{I_1, I_2, \dots, I_n\}$, and a text-to-image (T2I) diffusion model, we condition the model using different prompts throughout the denoising process. At each timestep t , we apply the prompt p_i such that $t \in I_i$. By aligning each proxy prompt with its interval, the denoising process is guided by concepts appropriate to the level of detail emerging at that stage. This enables gradual image construction while avoiding conflicts with the model’s learned priors. The injection mechanism integrates seamlessly into existing inference pipelines without architectural modifications and is compatible with a range of pretrained diffusion models.

5. Experiments and Results

In this section, we evaluate SAP through qualitative (Section 5.1) and quantitative (Section 5.2) comparisons. We further conduct ablation studies (Section 5.3) on component contributions and robustness, followed by a discussion on the limitations of our method.

Implementation Details. We use FLUX.1 [dev] [17] as the base T2I model and GPT-4o [1] for prompt decomposition. In all experiments, inference is performed using $T = 50$ steps and the LLM is restricted to at most three proxies per prompt. Baseline hyperparameters follow their original papers or implementations, with $T = 50$ steps for fair comparison. To further demonstrate robustness, we also report results with SD3.0 using the same LLM-generated proxy prompts and intervals.

Baselines. We compare SAP against the following approaches: (1) base models FLUX-dev (denoted by FLUX) [17] and SD3.0 [11]; (2) R2F [22], a training-



Figure 6. *Early insertion of the foreground allows the model to allocate more space to it, while late insertion confines the object within the existing layout, making it appear smaller (e.g., the snowman introduced at Step 5). Step labels indicate when the foreground object is introduced.*

free method reported under three settings: SD3.0 (original), FLUX-schnell (official), and our reimplementation on FLUX; (3) Annealing Guidance [34], which trains a small MLP to predict the classifier-free guidance scale at each step; and (4) Ella [16], a fine-tuned model on SD1.5. (5) VL-DNP [8], a VLM-guided negative prompting method, evaluated using SD3 with Qwen2.5-VL-7B.

Datasets We evaluate SAP using three datasets: Whoops! [7], Whoops-Hard, and ContraBench. *Whoops!* consists of 500 prompts paired with commonsense-defying images, designed to test visual reasoning and compositional understanding. While relevant to our task, many of its prompts are relatively easy for modern T2I models and do not consistently expose model limitations.

To address this, we curate *Whoops-Hard*, a subset of 100 particularly difficult prompts from *Whoops!*, providing a stronger benchmark for evaluating current state-of-the-art models. To further probe semantic alignment under contradictory conditions, we introduce *ContraBench*, a curated set of 40 prompts capturing contextual contradictions. The dataset was constructed in two steps: (1) ChatGPT generated candidate prompts based on the definition of contextual contradictions, and (2) human annotators filtered them to retain only those that clearly expressed contradictions. The full prompt lists for both datasets are provided in the Appendix.

5.1. Qualitative Results

Figure 8 presents qualitative comparisons on the Whoops! and ContraBench datasets (see Appendix for more results). Across both benchmarks, baseline methods consistently ex-



Figure 7. *Effect of interval assignment. Introducing the full prompt too early fails to disentangle contextual contradictions, while introducing it too late alters only fine details. Top proxy: “A pillow fort in a bedroom”; bottom proxy “A mother duck guards three ducklings”.*

hibit characteristic failure modes when handling contradictory prompts. In contrast, SAP successfully generates challenging cases such as a blue Shrek or a monkey juggling tiny elephants (Figure 8). In addition to FLUX, SAP also improves SD3 generations under contradictory prompts (Figure 9).

For SD3 and FLUX, contradictory prompts expose conflicts with learned priors, resulting in prompt misalignment. Ella and Annealing Guidance, not designed for contradictions, perform less effectively on such cases. R2F alternates between prompts at predefined timesteps, a strategy designed for attribute binding rather than addressing contextual contradictions. While it can reinforce rare concepts, it does not align prompts with the stages at where semantic features emerge during denoising. As a result, it often produces hybrid concepts that merge incompatible elements from conflicting concept (see the bodybuilder in Figure 9, and the owl and SpongeBob results in the Appendix).

In contrast, SAP produces semantically coherent outputs by introducing proxy prompts at denoising stages where corresponding features emerge. This enables effective handling of conflicting concepts. Across both benchmarks, SAP consistently generates coherent images for contradictory prompts. Robustness is further demonstrated in the Appendix, comparing generations across multiple seeds.

5.2. Quantitative Results

We evaluate prompt alignment using GPT-4o vision-language model (VLM). For each generated image, GPT-4o assigns a score from 1–5 based on adherence to the prompt. Scores are averaged across three fixed random



Figure 8. *Qualitative comparison of SAP with baseline methods. Our method resolves contextual contradictions, whereas baselines struggle to produce text-aligned images. Additional examples are provided in the Appendix.*



Figure 9. *SAP is robust to the base model, as shown by the results obtained with SAP_{SD3} .*

seeds per prompt and scaled to 20–100. The evaluation prompt is provided in the Appendix.

As shown in Table 1, SAP outperforms all baselines across the three benchmarks. Between the base models, SD3.0 tends to yield stronger alignment under contradictions, while FLUX offers higher visual quality (Figure 8). SAP improves both backbones, enhancing prompt adherence while maintaining the visual fidelity of the underlying models (Figures 8 and 9).

User study. VLM-based metrics often miss subtle semantic inconsistencies and do not adequately assess image quality. To complement them, we conducted a user study evaluating both prompt adherence and overall visual appearance.

We randomly sampled 24 prompts from the Whoops! and ContraBench benchmarks. For each prompt, participants compared two images, one generated by SAP and the other by a baseline, and answered: (1) which most accurately reflected the prompt, and (2) which had higher visual quality. In total, we collected responses from 61 users, yielding 1,464 individual evaluations. Table 2 summarizes the win rates of SAP against each baseline.

These results highlight the superiority of our approach in handling contextually contradictory prompts, achieving both stronger prompt alignment and higher visual quality.

5.3. Ablation Studies

We evaluate SAP through ablations that assess design choices in prompt decomposition and robustness under different conditions, such as timestep perturbations. Additional results on alternative LLMs and non-contradictory prompts are in the Appendix.

Prompt decomposition components. We conduct ablations on the Whoops-Hard benchmark, where each variant isolates a design choice to quantify its effect on alignment within our method (Table 3). In-context examples significantly improve the LLM’s ability to decompose contradictory prompts, leading to better text–image alignment. Removing the explanation requirement impairs reasoning and causes a notable drop, showing that generating explicit explanations encourages more coherent semantic decisions. Restricting decomposition to two proxies performs close to the full method, while allowing up to three proxies provides

Table 1. *Quantitative evaluation on various benchmarks using the GPT-4o vision-language model. We report average alignment, where alignment reflects how well the image matches the prompt semantics, independent of visual quality. SAP achieves the best results, regardless of the base model.*

Models	Benchmarks		
	Whoops	Whoops-Hard	Contra-Bench
SD3.0	82.63	55.73	57.5
FLUX	78.85	44.3	57.16
Ella	69.09	45.19	55.16
Annealing	79.59	59.06	58.33
VL-DNP	82.79	56.26	58.83
R2F	83.50	57.06	59.16
R2F _{schne} ll	79.58	54.80	59.33
R2F _{FLUX}	48.68	32.80	25.33
SAP _{SD3.0}	85.87	64.40	65.33
SAP	<u>85.10</u>	<u>62.13</u>	66.16

Table 2. *User study results. Win rates of SAP in text-image alignment and image quality, compared against each baseline method.*

	SD3	FLUX	Ella	Annealing	R2F
Alignment	70%	81%	81%	73%	75%
Quality	72%	63%	74%	79%	68%

Table 3. *Ablation on Whoops-Hard. We evaluate our prompt decomposition method by (1) removing in-context examples, (2) removing the explanation requirement, and (3) limiting decomposition to two proxy prompts.*

		w/o static	w/o in-context reasoning	2 proxy	Full
Alignment	44.3	48.0	46.46	60.26	62.13

extra flexibility for harder cases and yields further gains.

Robustness to LLM-predicted timestep intervals. Our method relies on LLM-predicted intervals to schedule proxy prompts, but these boundaries do not require exact placement. The earlier results (Figure 7) highlight that placing proxy prompts at the wrong *stage* of denoising (e.g., too early or too late) can harm alignment. Here we show that within the correct coarse stage, the method is robust to moderate boundary shifts. Specifically, we perturb interval boundaries while keeping the proxy prompts fixed, uniformly shifting them within windows of varying size. As shown in Table 4, small shifts of up to ± 1 step (window=3) have almost no effect on alignment, and even larger shifts of up to ± 2 steps (window=5) cause only minor degradation, despite representing a substantial perturbation relative to the full method effective range (~ 12 steps; see Appendix). These results confirm that SAP is sensitive to the stage at which information is introduced, but largely insensitive to exact step boundaries within that stage.



Figure 10. Failure cases of SAP.

Table 4. *Effect of perturbing LLM-predicted timestep intervals. Boundaries are uniformly shifted within window w . $SAP_{w=i}$ denotes evaluation with window i .*

Models	Benchmarks		
	Whoops	Whoops-Hard	Contra-Bench
FLUX	78.85	44.3	57.16
SAP	85.10	62.13	66.16
SAP _{w=3}	84.18	62.06	65.5
SAP _{w=5}	81.46	58.46	62.5

Limitations. In Figure 10, we present representative failure cases of our method on examples from the Whoops! benchmark. Since our approach relies on guiding the model through text alone, it cannot control properties that the underlying model inherently struggles with, such as generating specific quantities or enforcing precise orientations; a more detailed categorization and analysis of failure modes is provided in the supplementary.

6. Conclusions

We introduced a training-free framework for resolving contextual contradictions in text-to-image generation, cases where seemingly plausible prompts fail due to strong, hidden model biases. At its core, our method leverages the coarse-to-fine generation process to separate contradictions across denoising stages, enabling faithful rendering of prompts that would otherwise yield semantically inconsistent outputs. The introduction of proxy prompts steers the generative process in line with the model’s priors, enabling it to resolve conflicts and preserve semantic fidelity without the need for retraining or fine-tuning.

We argue that since our approach already leverages the broad world knowledge of vision–language models, integrating them more tightly with generative models holds promise for addressing contextual contradictions directly. As a next step, we plan to explore emerging compound architectures that combine VLMs and generative models, with the aim of understanding how to effectively harness them to resolve conflicts in open-ended generation.

Acknowledgments

This research was supported in part by the Israel Science Foundation (grants no. 2492/20 and 1473/24), Len Blavatnik and the Blavatnik family foundation.

References

- [1] Josh Achiam, Steven Adler, Sandhini Agarwal, Lama Ahmad, Ilge Akkaya, Florencia Leoni Aleman, Diogo Almeida, Janko Altschmidt, Sam Altman, Shyamal Anadkat, et al. Gpt-4 technical report. *arXiv preprint arXiv:2303.08774*, 2023. 5
- [2] Aishwarya Agarwal, Srikrishna Karanam, KJ Joseph, Apoorv Saxena, Koustava Goswami, and Balaji Vasani. A-star: Test-time attention segregation and retention for text-to-image synthesis. In *Proceedings of the IEEE/CVF International Conference on Computer Vision*, pages 2283–2293, 2023. 2
- [3] Yuval Alaluf, Elad Richardson, Gal Metzger, and Daniel Cohen-Or. A neural space-time representation for text-to-image personalization. *ACM Transactions on Graphics (TOG)*, 42(6):1–10, 2023. 2
- [4] Yogesh Balaji, Seungjun Nah, Xun Huang, Arash Vahdat, Jiaming Song, Qinsheng Zhang, Karsten Kreis, Miika Aittala, Timo Aila, Samuli Laine, et al. ediff-i: Text-to-image diffusion models with an ensemble of expert denoisers. *arXiv preprint arXiv:2211.01324*, 2022. 2, 4
- [5] Omer Bar-Tal, Lior Yariv, Yaron Lipman, and Tali Dekel. Multidiffusion: Fusing diffusion paths for controlled image generation. 2023. 3
- [6] Sara Beery, Grant Van Horn, and Pietro Perona. *Recognition in Terra Incognita*, page 472–489. Springer International Publishing, 2018. 2
- [7] Nitzan Bitton-Guetta, Yonatan Bitton, Jack Hessel, Ludwig Schmidt, Yuval Elovici, Gabriel Stanovsky, and Roy Schwartz. Breaking common sense: Whoops! a vision-and-language benchmark of synthetic and compositional images. In *2023 IEEE/CVF International Conference on Computer Vision (ICCV)*, page 2616–2627. IEEE, 2023. 2, 6
- [8] Hoyeon Chang, Seungjin Kim, and Yoonseok Choi. Dynamic vlm-guided negative prompting for diffusion models. *arXiv preprint arXiv:2510.26052*, 2025. 6
- [9] Hila Chefer, Yuval Alaluf, Yael Vinker, Lior Wolf, and Daniel Cohen-Or. Attend-and-excite: Attention-based semantic guidance for text-to-image diffusion models. *ACM transactions on Graphics (TOG)*, 42(4):1–10, 2023. 2, 4
- [10] Omer Dahary, Or Patashnik, Kfir Aberman, and Daniel Cohen-Or. Be yourself: Bounded attention for multi-subject text-to-image generation. In *European Conference on Computer Vision*, pages 432–448. Springer, 2024. 2
- [11] Patrick Esser, Sumith Kulal, Andreas Blattmann, Rahim Entezari, Jonas Müller, Harry Saini, Yam Levi, Dominik Lorenz, Axel Sauer, Frederic Boesel, et al. Scaling rectified flow transformers for high-resolution image synthesis. In *Forty-first international conference on machine learning*, 2024. 5
- [12] Weixi Feng, Xuehai He, Tsu-Jui Fu, Varun Jampani, Arjun Akula, Pradyumna Narayana, Sugato Basu, Xin Eric Wang, and William Yang Wang. Training-free structured diffusion guidance for compositional text-to-image synthesis. *arXiv preprint arXiv:2212.05032*, 2022. 2
- [13] Robert Geirhos, Jörn-Henrik Jacobsen, Claudio Michaelis, Richard Zemel, Wieland Brendel, Matthias Bethge, and Felix A. Wichmann. Shortcut learning in deep neural networks. *Nature Machine Intelligence*, 2(11):665–673, 2020. 2
- [14] Amir Hertz, Ron Mokady, Jay Tenenbaum, Kfir Aberman, Yael Pritch, and Daniel Cohen-Or. Prompt-to-prompt image editing with cross attention control. *arXiv preprint arXiv:2208.01626*, 2022. 4
- [15] Jonathan Ho, Ajay Jain, and Pieter Abbeel. Denoising diffusion probabilistic models. *arXiv preprint arxiv:2006.11239*, 2020. 1
- [16] Xiwei Hu, Rui Wang, Yixiao Fang, Bin Fu, Pei Cheng, and Gang Yu. Ella: Equip diffusion models with llm for enhanced semantic alignment. *arXiv preprint arXiv:2403.05135*, 2024. 3, 6
- [17] Black Forest Labs. Flux. <https://github.com/black-forest-labs/flux>, 2024. 5
- [18] Jun Hao Liew, Hanshu Yan, Daquan Zhou, and Jiashi Feng. Magicmix: Semantic mixing with diffusion models. *arXiv preprint arXiv:2210.16056*, 2022. 3
- [19] Nan Liu, Shuang Li, Yilun Du, Antonio Torralba, and Joshua B Tenenbaum. Compositional visual generation with composable diffusion models. In *European Conference on Computer Vision*, pages 423–439. Springer, 2022. 3
- [20] Tom McCoy, Ellie Pavlick, and Tal Linzen. Right for the wrong reasons: Diagnosing syntactic heuristics in natural language inference. In *Proceedings of the 57th Annual Meeting of the Association for Computational Linguistics*. Association for Computational Linguistics, 2019. 2
- [21] Tuna Han Salih Meral, Enis Simsar, Federico Tombari, and Pinar Yanardag. Conform: Contrast is all you need for high-fidelity text-to-image diffusion models. In *Proceedings of the IEEE/CVF Conference on Computer Vision and Pattern Recognition*, pages 9005–9014, 2024. 2
- [22] Dongmin Park, Sebin Kim, Taehong Moon, Minkyu Kim, Kangwook Lee, and Jaewoong Cho. Rare-to-frequent: Unlocking compositional generation power of diffusion models on rare concepts with llm guidance. *arXiv preprint arXiv:2410.22376*, 2024. 3, 5
- [23] Or Patashnik, Daniel Garibi, Idan Azuri, Hadar Averbuch-Elor, and Daniel Cohen-Or. Localizing object-level shape variations with text-to-image diffusion models. In *Proceedings of the IEEE/CVF international conference on computer vision*, pages 23051–23061, 2023. 2, 3, 4
- [24] Aditya Ramesh, Mikhail Pavlov, Gabriel Goh, Scott Gray, Chelsea Voss, Alec Radford, Mark Chen, and Ilya Sutskever. Zero-shot text-to-image generation, 2021. 1
- [25] Royi Rassin, Shauli Ravfogel, and Yoav Goldberg. Dalle-2 is seeing double: Flaws in word-to-concept mapping in text2image models. *arXiv preprint arXiv:2210.10606*, 2022. 2

- [26] Royi Rassin, Eran Hirsch, Daniel Glickman, Shauli Ravfogel, Yoav Goldberg, and Gal Chechik. Linguistic binding in diffusion models: Enhancing attribute correspondence through attention map alignment. *Advances in Neural Information Processing Systems*, 36:3536–3559, 2023. [2](#)
- [27] Robin Rombach, Andreas Blattmann, Dominik Lorenz, Patrick Esser, and Björn Ommer. High-resolution image synthesis with latent diffusion models. In *Proceedings of the IEEE/CVF conference on computer vision and pattern recognition*, pages 10684–10695, 2022. [1](#)
- [28] Krishna Kumar Singh, Dhruv Mahajan, Kristen Grauman, Yong Jae Lee, Matt Feiszli, and Deepti Ghadiyaram. Don’t judge an object by its context: Learning to overcome contextual bias. In *2020 IEEE/CVF Conference on Computer Vision and Pattern Recognition (CVPR)*. IEEE, 2020. [2](#)
- [29] Hazarapet Tunanyan, Dejjia Xu, Shant Navasardyan, Zhangyang Wang, and Humphrey Shi. Multi-concept t2i-zero: Tweaking only the text embeddings and nothing else. *arXiv preprint arXiv:2310.07419*, 2023. [2](#)
- [30] Andrey Voynov, Qinghao Chu, Daniel Cohen-Or, and Kfir Aberman. p+: Extended textual conditioning in text-to-image generation. *arXiv preprint arXiv:2303.09522*, 2023. [2](#)
- [31] Kai Yuanqing Xiao, Logan Engstrom, Andrew Ilyas, and Aleksander Madry. Noise or signal: The role of image backgrounds in object recognition. In *International Conference on Learning Representations*, 2021. [2](#)
- [32] Ling Yang, Zhaochen Yu, Chenlin Meng, Minkai Xu, Stefano Ermon, and Bin Cui. Mastering text-to-image diffusion: Recaptioning, planning, and generating with multi-modal llms. In *Forty-first International Conference on Machine Learning*, 2024. [3](#)
- [33] Wenqian Ye, Guangtao Zheng, Xu Cao, Yunsheng Ma, and Aidong Zhang. Spurious correlations in machine learning: A survey. *arXiv preprint arXiv:2402.12715*, 2024. [2](#)
- [34] Shai Yehezkel, Omer Dahary, Andrey Voynov, and Daniel Cohen-Or. Navigating with annealing guidance scale in diffusion space. *arXiv preprint arXiv:2506.24108*, 2025. [2](#), [6](#)

Image Generation from Contextually Contradictory Prompts

Supplementary Material

7. Ethics Statement

Our work contributes to improving the semantic alignment of text-to-image models under contradictory or biased prompts. As a consequence, our method enhances users’ ability to control generative models and faithfully render contradictory concepts. While this provides positive benefits, such as reducing unintended biases and enabling more inclusive image generation, it also increases the potential for misuse, including the creation of harmful, misleading, or inappropriate content. As with any advance in generative modeling, these dual-use concerns highlight the importance of responsible deployment, safeguards, and continued ethical oversight to ensure that such improvements contribute positively to society.

8. Additional Results

Robustness across LLMs. Since our framework hinges on LLM-driven prompt decomposition, we further examined its robustness under different language models. We evaluated both a proprietary model (GPT-4o) and a comparatively lightweight open-source alternative (LLaMA-3.1-8B-Instruct). While GPT-4o delivers the strongest performance, the smaller LLaMA-3.1-8B-Instruct still yields consistent improvements over the baseline (see Table 5).

Improved realism. SAP generates photorealistic and semantically coherent images for prompts with atypical attribute combinations (Figure 11). In contrast, FLUX often defaults to cartoon-like renderings, even when photorealism is explicitly requested, revealing a contextual contradiction between fantastical content and realistic style. By using contradiction-free proxy prompts, SAP avoids these biases and produces realistic outputs regardless of whether photorealism is explicitly required in the prompt.

Non-contradictory prompts. To ensure applicability in general text-to-image scenarios, we verify that our method does not negatively affect prompts without contextual contradictions. We find that including even a single non-contradictory in-context example is sufficient for the LLM to default to using the full prompt in such cases. We evaluate this behavior using GPT-4o alignment scores on the PartiPrompts-Simple benchmark, which contains simple, non-contradictory prompts (Table 6).

Additional qualitative comparisons. Figures 13 and 14 present additional qualitative comparisons of our method, while Figure 15 shows results across multiple seeds.

Failure Mode Analysis. We analyze failure cases of SAP and group them into three categories, summarized in Table 7. The majority of failures arise from incorrect proxy prompt assignment, where the selected proxy does not adequately preserve the intended structure or semantics of the target concept. In many such cases, manually correcting the proxy resolves the contradiction, as illustrated in Figure 12 (left), indicating that these failures stem

Table 5. Performance of SAP when combined with different LLMs, comparing GPT-4o and Llama-3.1-8B-Instruct.

Models	Benchmarks		
	Whoops	Whoops-Hard	Contra-Bench
FLUX	78.85	44.3	57.16
SAP _{GPT4o}	85.10	62.13	66.16
SAP _{Llama3.1}	80.52	59.53	61.16

Table 6. Alignment performance on the PartiPrompts-simple benchmark, which contains simple, non-contradictory prompts. Scores are computed using GPT-4o vision-language model. Our method achieves comparable performance to the base model, indicating no degradation on regular prompts.

Models	PartiPrompts-simple
FLUX	93.46
SAP	93.06



Figure 11. FLUX tends to generate realistic images by default. However, when given unrealistic prompts, it often produces cartoon-like samples. In contrast, our method, which gradually resolves such prompts through coherent proxy stages, consistently generates realistic and semantically aligned images.

from limitations of the LLM rather than the proposed framework, and can potentially be mitigated. A second group of failures stems from inherent limitations of the underlying diffusion model, such as difficulty generating an empty pool or rendering unusual symbolic structures (e.g., compass directions), which persist even with correct prompt decomposition (Figure 12, right). Finally, only a small fraction of failures is attributed to suboptimal interval assignment, consistent with our findings that SAP is robust to moderate variations in timestep scheduling.

Table 7. Breakdown of SAP failure cases by root cause.

	Interval assignment	Proxy assignment	Model limitation
Failure cases	3.3%	63.3%	33.3%



Figure 12. Failure cases of SAP. Left: a proxy assignment failure, where an unsuitable proxy leads to incorrect generation; manually correcting the proxy (right image in pair) resolves the contradiction. Right: failures due to inherent limitations of the underlying diffusion model, such as difficulty generating an empty pool or rendering unusual symbolic structures (e.g., a compass with incorrect directions).

Computational Overhead. SAP introduces modest overhead due to a single LLM inference for prompt decomposition, performed once per prompt prior to diffusion, and a lightweight additional embedding pass. As this step occurs only once and is independent of the denoising process, it does not significantly impact overall generation time.

9. LLM Instruction for Prompt Decomposition

Tables 8 and 9 detail the full LLM instruction used for our method’s decomposition, along with the corresponding in-context examples. In a single inference pass, our method detects contextual contradictions, generates proxy prompts, and assigns timestep intervals.

Table 10 presents examples of our LLM input prompts, along with the corresponding output explanations and the decomposition into proxy prompts and timestep intervals.

10. Provided Benchmarks

We describe the construction of *ContraBench* and *Whoops-Hard* in the main text. Here, we provide the full lists of prompts for these benchmarks in Table 11 and Table 12, respectively.

11. VLM Evaluation

We utilize GPT-4o to assess alignment between prompts and their generated images. The instruction prompt provided to the VLM is shown in Table 13.

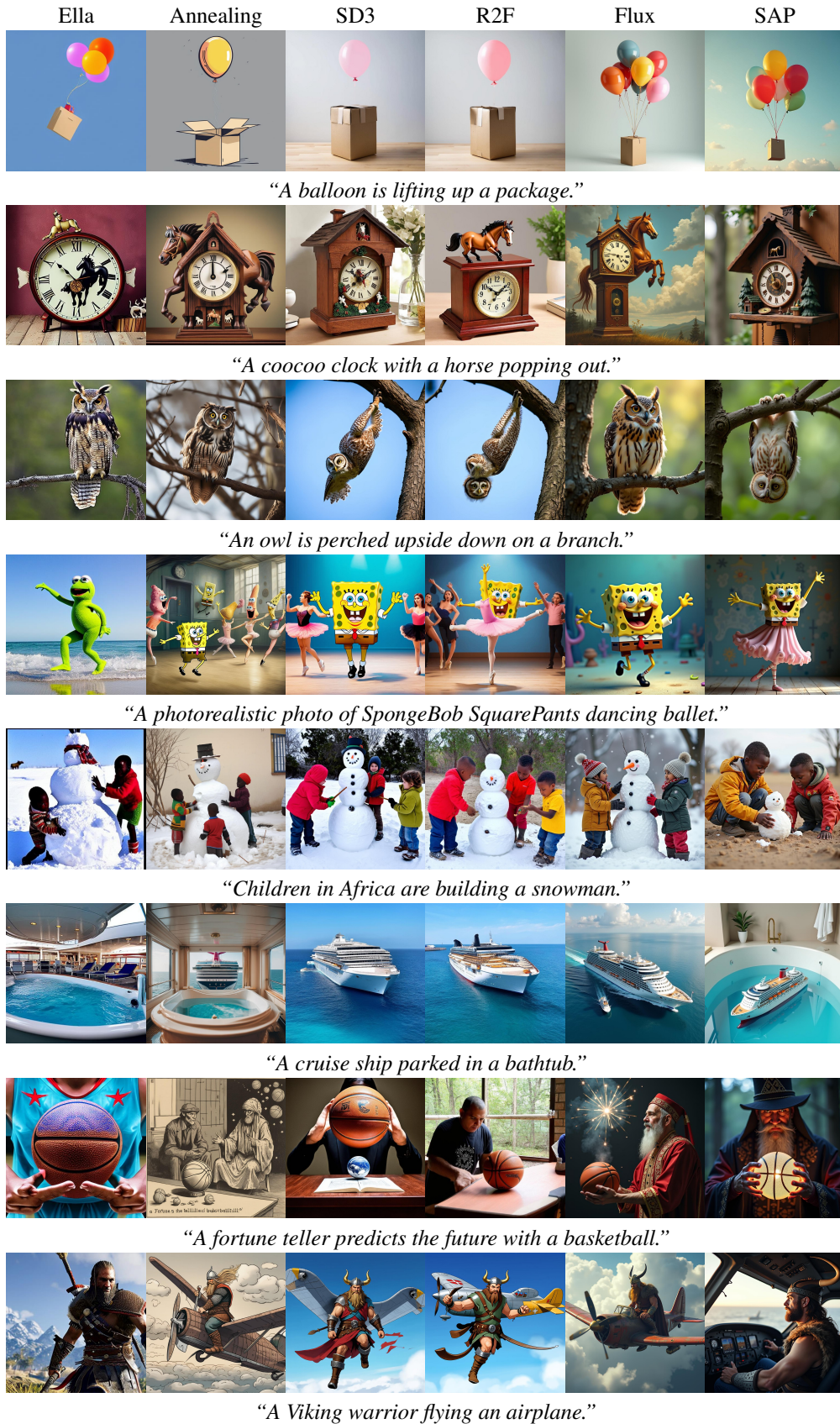


Figure 13. *Qualitative comparison. Our method consistently generates text-aligned images for contextually contradicting prompts.*

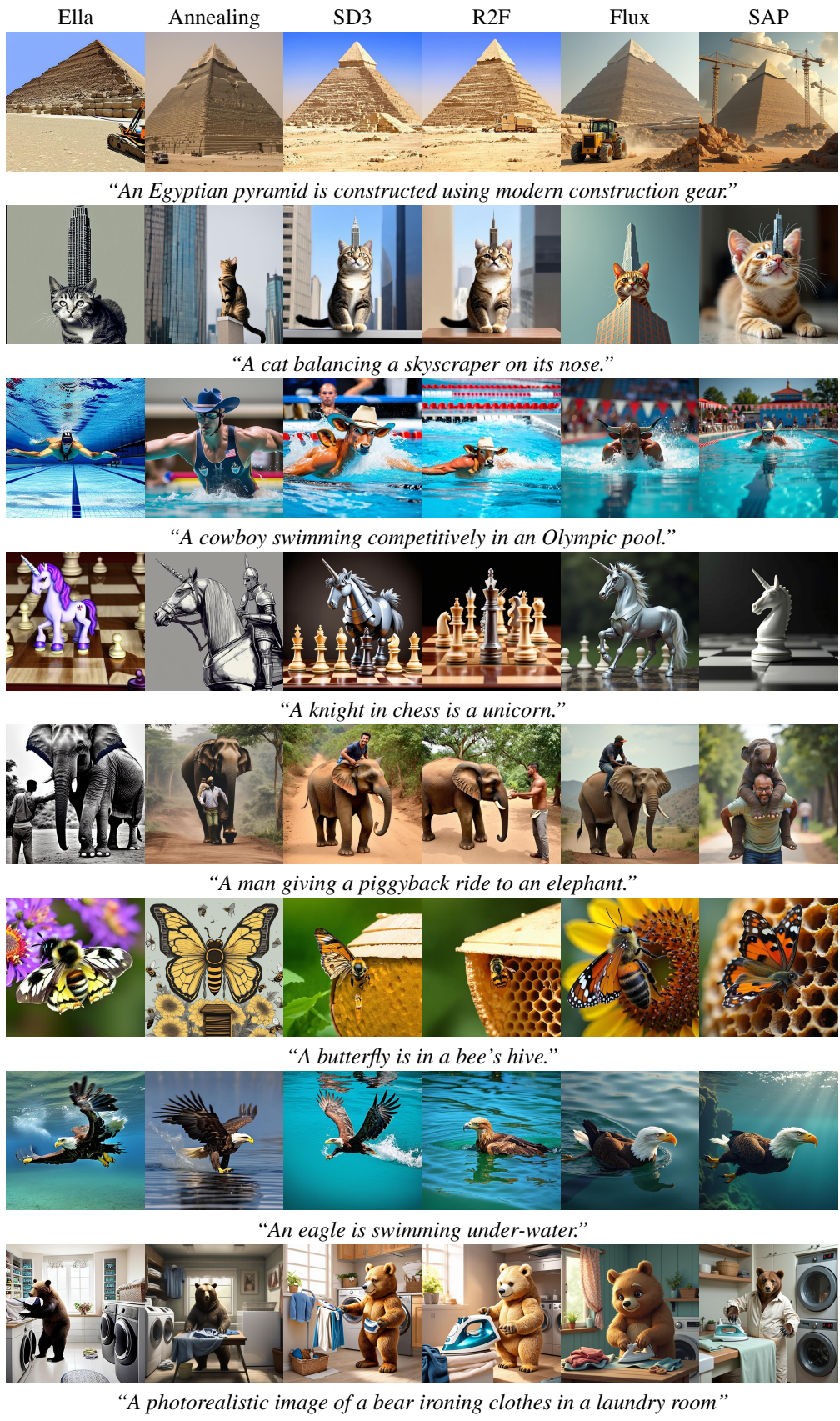


Figure 14. *Qualitative comparison. Our method consistently generates text-aligned images for contextually contradicting prompts.*

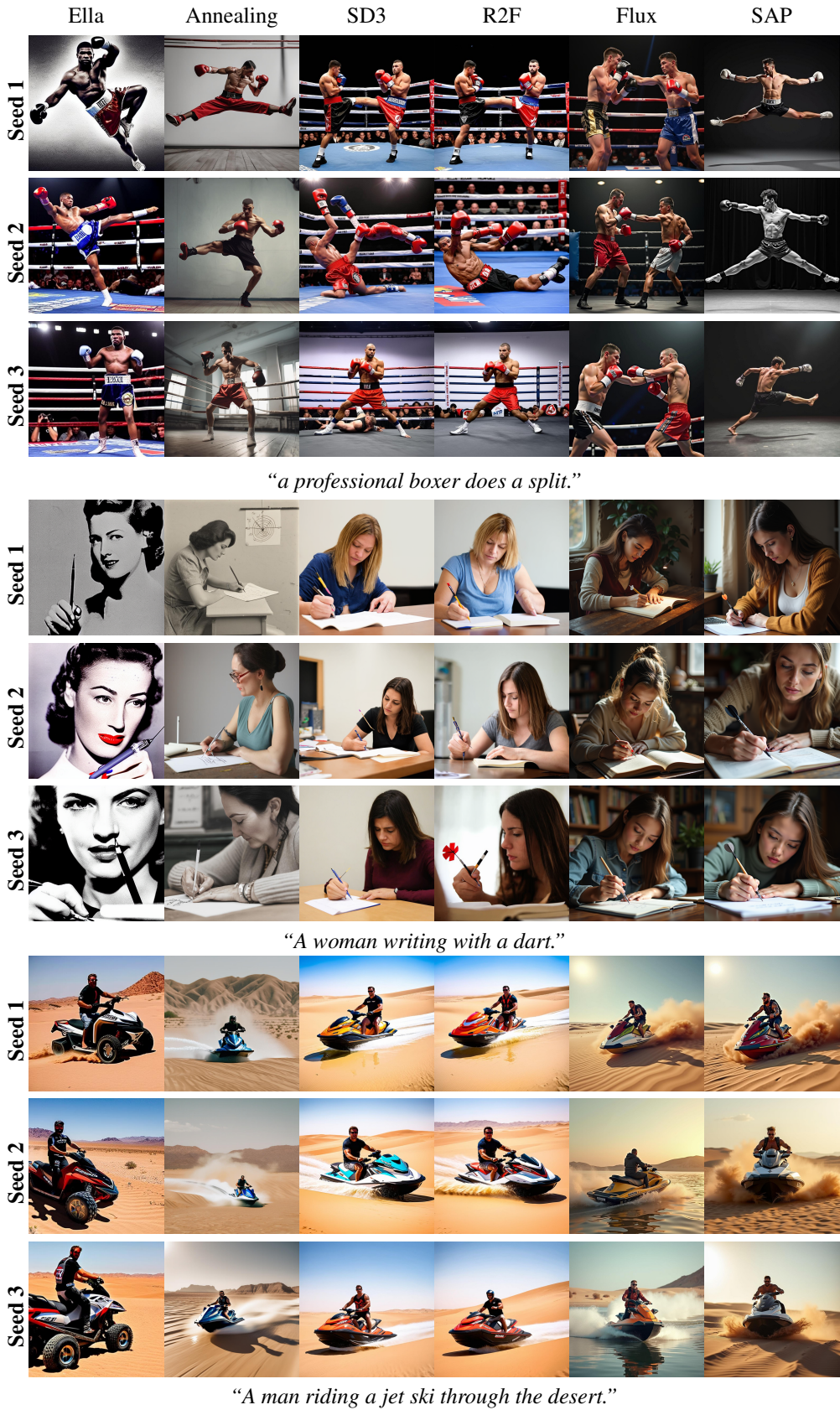


Figure 15. Qualitative comparison across multiple seeds. Our method consistently generates text-aligned images for contextually contradicting prompts.

Table 8. Full LLM prompt instruction SAP, used to decompose prompts by denoising stages.

<System Prompt>

You are an expert assistant in time step dependent prompt conditioning for diffusion models.

Your task is to decompose a complex or contextually contradictory prompt into up to **three** intermediate prompts that align with the model’s denoising stages — from background layout to object identity to fine detail. Only introduce prompt transitions when needed.

Diffusion Semantics (Low → High Frequency Progression):

Steps 0–2: Scene layout and dominant color regions (e.g., sky, forest, sand tone)

Steps 3–6: Object shape, size, pose, and position

Steps 7–10: Object identity, material, and surface type (e.g., glass vs. rubber)

Steps 11–13+: Fine features and local details (e.g., tattoos, insects, facial detail)

Since denoising progresses from coarse to fine, it is crucial to stabilize large-scale visual structures (such as body shape, pose, and background) before introducing small or semantically charged elements (such as facial details, objects in hand, or surreal features).

Substitution Strategy:

1. Begin with high-level layout (background, geometry).
2. Use **placeholder concepts** if needed to stabilize layout before detailed insertions.
3. Substitutes must match in shape, size, and visual function.
4. Replace placeholders as soon as fidelity permits.
5. Do not maintain substitutions longer than needed.
6. If the prompt is visually coherent, return a **single prompt** with no decomposition.

Output Format:

a. Explanation: A short sentence explaining why decomposition is needed.

b. Final dictionary:

```
{
  "prompts_list": [
    "<prompt1>",
    "<prompt2>",
    "...",
    "<target prompt>"
  ],
  "switch_prompts_steps": [<step1>, <step2>, ...]
}
```

- The length of switch_ prompts_steps should be one less than prompts_list.

- Do not include any text outside this structure.

Table 9. *In-context examples SAP, illustrating reasoning steps and prompt decomposition across denoising stages.*

Input: A polar bear in a desert

Output:

- a. Explanation: A polar bear is common in snowy scenes, not deserts. Since no suitable object proxy exists, the prompt starts with the desert alone before introducing the unlikely animal.
- b. Final dictionary:

```
{
  "prompts_list": [
    "A desert",
    "A polar bear in a desert"
  ],
  "switch_prompts_steps": [2]
}
```

Input: A fox in a nursery

Output:

- a. Explanation: A fox is uncommon in indoor scenes. Starting with a dog, then a visually similar breed (Shiba Inu), provides a natural proxy before introducing the fox in a childlike setting.
- b. Final dictionary:

```
{
  "prompts_list": [
    "A dog in a nursery",
    "A Shiba Inu dog in a nursery",
    "A fox in a baby room"
  ],
  "switch_prompts_steps": [4, 7]
}
```

Input: A shoes tree in the meadow

Output:

- a. Explanation: Treating a “shoes tree” like an “apple tree” allows the model to build structure and object layout using familiar patterns. Introducing apples first grounds the scene in a biologically plausible layout before shifting to the surreal concept of shoes as fruit-like objects.
- b. Final dictionary:

```
{
  "prompts_list": [
    "tree in the meadow",
    "A tree full of apples, in the meadow",
    "A tree full of shoes in the meadow"
  ],
  "switch_prompts_steps": [4,8]
}
```

Input: A red sports car parked on a mountain road

Output:

- a. Explanation: This is a realistic and visually coherent scene, so no decomposition is needed.
- b. Final dictionary:

```
{
  "prompts_list": [
    "A red sports car parked on a mountain road"
  ],
  "switch_prompts_steps": []
}
```

Table 10. *Prompt decompositions of contradictory prompts using SAP.*

Original Prompt	Explanation	Prompt Sequence	Switch Step(s)
A grown man has a baby’s pacifier in his mouth.	The grown man is established first for structure, while the pacifier, being a small but semantically significant detail, is added once the main identity is resolved.	1. A grown man with a small object in his mouth 2. A grown man has a baby’s pacifier in his mouth	4
A dragon is blowing water.	Dragons are more commonly depicted blowing fire. A proxy of white smoke is visually similar to water mist in texture, stabilizing the emission process before resolving the surreal water emission.	1. A dragon blowing white smoke 2. A dragon blowing water	3
A pizza with grape toppings.	Pizza with traditional toppings stabilizes the geometry and color before introducing the visually similar yet unusual grape topping.	1. A pizza with pepperoni toppings 2. A pizza with grape toppings	3
A coin floats on the surface of the water.	Coins typically sink in water, not float. Starting with a leaf—an object that naturally floats—ensures that this behavior within the scene is handled correctly before introducing the coin.	1. A leaf floats on the surface of the water 2. A coin floats on the surface of the water	4
A cockatoo parrot swimming in the ocean.	Cockatoos are birds and naturally do not swim; starting with a simple bird on water stabilizes position and motion. Progressing to a duck, before introducing the cockatoo parrot, eases the transition into the final surreal visual.	1. A duck swimming in the ocean 2. A parrot swimming in the ocean 3. A cockatoo parrot swimming in the ocean	3, 6
Shrek is blue.	Shrek is a distinct character with a recognizable green color. Using a simple blue ogre initially sets the stage for a color change before fully introducing Shrek to ensure visual coherence.	1. A blue ogre 2. Shrek is blue	3
A professional boxer does a split.	Professional boxers are typically shown in athletic stances related to fighting, not performing a split. Starting with a gymnast performing a split supports the action, introducing a boxer in similar attire balances identity shift without disrupting the pose.	1. A gymnast performing a split 2. A boxer performing a split 3. A professional boxer doing a split	3, 6

Table 11. *ContraBench. A curated benchmark of 40 contradictory prompts for evaluating text-to-image models.*

ID	Prompt	ID	Prompt
1	A professional boxer does a split	21	A mosquito pulling a royal carriage through Times Square
2	A bear performing a handstand in the park	22	A grandma is ice skating on the roof
3	A bodybuilder balancing on point shoes	23	A baseball player backswing a yellow ball with a golf club
4	A chicken is smiling	24	A house with a circular door
5	A cruise ship parked in a bathtub	25	A photorealistic image of a bear ironing clothes in a laundry room
6	A man giving a piggyback ride to an elephant	26	A pizza being used as an umbrella in the rain
7	A zebra climbing a tree	27	A cubist lion hiding in a photorealistic jungle
8	A coffee machine dispensing glitter	28	A cowboy swimming competitively in an Olympic pool
9	A vending machine in a human running posture	29	A realistic photo of an elephant wearing slippers
10	A ballerina aggressively flipping a table	30	A computer mouse eating a piece of cheese
11	A bathtub floating above a desert in a tornado	31	A horse taking a selfie with a smartphone
12	A monkey juggles tiny elephants	32	A sheep practicing yoga on a mat
13	A woman has a marine haircut	33	A snake eating a small golden guitar
14	A tower with two hands	34	A soccer field painted on a grain of rice
15	An archer is shooting flowers with a bow	35	A snake with feet
16	A muscular ferret in the woods	36	A woman brushing her teeth with a paintbrush
17	A barn built atop a skyscraper rooftop	37	A horse with a hump
18	A cat balancing a skyscraper on its nose	38	A hyperrealistic unicorn made of origami
19	A cow grazing on a city rooftop	39	A library printed on a butterfly’s wings
20	A fireplace burning inside an igloo	40	A photorealistic photo of SpongeBob SquarePants dancing ballet

Table 12. *Whoops-Hard*. A curated subset of 100 challenging prompts from the *Whoops!* benchmark.

ID	Prompt	ID	Prompt
1	A bouquet of flowers is upside down in a vase	51	A Japanese tea ceremony uses coffee instead of tea
2	A man is welding without a mask	52	A wagon is being pushed from behind by two opposite facing horses
3	A man eats hamburgers in a baby chair	53	The Girl with a Pearl Earring wears a golden hoop earring
4	A turn right street sign with a left turn arrow	54	A chandelier is hanging low to the ground
5	Goldilocks sleeps with four bears	55	The portrait of the Mona Lisa depicts a stern male face
6	A cake wishes a happy 202nd birthday	56	A car with the steering wheel right in the middle of the dashboard
7	Children are unhappy at Disneyland	57	A pagoda sits in front of the Eiffel Tower
8	An orange carved as a Jack O'Lantern	58	A man without protection next to a swarm of bees
9	A pen is being sharpened in a pencil sharpener	59	A kiwi bird in a green bamboo forest
10	Steve Jobs demonstrating a Microsoft tablet	60	The Sphinx is decorated like a sarcophagus outside a Mayan temple
11	Shrek is blue	61	A butterfly is in a bee's hive
12	A MacBook with a pear logo on it	62	A rainbow colored tank
13	A woman hits an eight ball with a racket	63	Movie goers nibble on vegetables instead of popcorn
14	Vikings ride on public transportation	64	A grown man has a baby's pacifier in his mouth
15	A gift wrapped junked car	65	A full pepper shaker turned upside down with nothing coming out
16	A rainbow is filling the stormy sky at night	66	The Tiger King, Joe Exotic, poses with an adult saber-tooth tiger
17	John Lennon using a MacBook	67	A scale is balanced with one side full and the other empty
18	Michelangelo's David is covered by a fig leaf	68	A pizza box is full of sushi
19	Chuck Norris struggles to lift weights	69	A man wearing a dog recovery cone collar while staring at his dog
20	Paratroopers deploy out of hot air balloons	70	A woman's mirror reflection is wearing different clothes
21	A train on asphalt	71	A woman using an umbrella made of fishnet in the rain
22	Lionel Messi playing tennis	72	A field of sunflowers with pink petals
23	A man jumping into an empty swimming pool	73	An eagle swimming under water
24	An airplane inside a small car garage	74	A woman stands in front of a reversed reflection in a mirror
25	An upside down knife about to slice a tomato	75	Stars visible in the sky with a bright afternoon sun
26	Dirty dishes in a bathroom sink	76	A car with an upside down Mercedes-Benz logo
27	A roulette wheel used as a dart board	77	An owl perched upside down on a branch
28	A smartphone plugged into a typewriter	78	A man in a wheelchair ascends steps
29	A passenger plane parked in a parking lot	79	Bach using sound mixing equipment
30	Guests are laughing at a funeral	80	A steam train on a track twisted like a roller coaster
31	A cat chasing a dog down the street	81	Roman centurions fire a cannon
32	The Statue of Liberty is holding a sword	82	A crab with four claws
33	A Rubik's cube with ten purple squares	83	Elon Musk wearing a shirt with a Meta logo
34	A girl roller skating on an ice rink	84	A compass with North South South West points
35	A butterfly swimming under the ocean	85	A glass carafe upside down with contents not pouring
36	Lightning striking a shack on a sunny day	86	Princess Diana standing in front of her grown son, Prince Harry
37	The Cookie Monster is eating apples	87	A children's playground set in the color black
38	A man is given a purple blood transfusion	88	A mug of hot tea with a plastic straw
39	An unpeeled banana in a blender	89	A whole pomegranate inside a corked glass bottle
40	A square apple	90	Belle from Beauty and the Beast about to kiss the Frog Prince
41	A place setting has two knives	91	A person's feet facing opposite directions
42	A koala in an Asian landscape	92	A bowl of cereal in water
43	A mouse eats a snake	93	A boy playing frisbee with a porcelain disk
44	A field of carrots growing above ground	94	A chef prepares a painting
45	A pregnant woman eating raw salmon	95	A dragon blowing water
46	A tiger staring at zebras in the savanna	96	The lip of a pitcher on the same side as the handle
47	Albert Einstein driving a drag racing car	97	Greta Thunberg holding a disposable plastic cup
48	A soccer player about to kick a bowling ball	98	A fortune teller predicting the future with a basketball
49	An old man riding a unicycle	99	A balloon lifting up a package
50	A hockey player drives a golf ball down the ice	100	Bruce Lee in a yellow leotard and tutu practicing ballet

Table 13. *VLM instruction for evaluation. Used by GPT-4o to score semantic alignment of generated images.*

You are an assistant evaluating an image on how well it aligns with the meaning of a given text prompt.

The text prompt is: "{prompt}"

PROMPT ALIGNMENT (Semantic Fidelity)

Evaluate only the *meaning* conveyed by the image — ignore visual artifacts.

Focus on:

- Are the correct objects present and depicted in a way that clearly demonstrates their intended roles and actions from the prompt?
- Does the scene illustrate the intended situation or use-case in a concrete and functional way, rather than through symbolic, metaphorical, or hybrid representation?
- If the described usage or interaction is missing or unclear, alignment should be penalized.
- Focus strictly on the presence, roles, and relationships of the described elements — not on rendering quality.

Score from 1 to 5:

- 5: Fully conveys the prompt’s meaning with correct elements
- 4: Mostly accurate — main elements are correct, with minor conceptual or contextual issues
- 3: Main subjects are present but important attributes or actions are missing or wrong
- 2: Some relevant components are present, but key elements or intent are significantly misrepresented
- 1: Does not reflect the prompt at all

Respond using this format:

```
### ALIGNMENT SCORE: <score>
### ALIGNMENT EXPLANATION: <explanation>
```
